

# Ground and excited state energy calculations of the H<sub>2</sub> molecule using a variational quantum eigensolver algorithm on an NMR quantum simulator

Dileep Singh,<sup>1,\*</sup> Shashank Mehendale,<sup>2,†</sup> Arvind,<sup>1,‡</sup> and Kavita Dorai<sup>1,§</sup>

<sup>1</sup>*Department of Physical Sciences, Indian Institute of Science Education & Research Mohali, Sector 81 SAS Nagar, Manauli PO 140306 Punjab, India.*

<sup>2</sup>*Department of Chemistry, University of Toronto, Toronto, ON M5S 1A1, Canada*

Variational quantum algorithms are emerging as promising candidates for near-term practical applications of quantum information processors, in the field of quantum chemistry. We implement the variational quantum eigensolver algorithm to calculate the molecular ground-state energy of the H<sub>2</sub> molecule and experimentally demonstrated it on an NMR quantum processor. Further, we simulate the excited states of the H<sub>2</sub> molecule using the variational quantum deflation algorithm and experimentally demonstrate it on the same NMR quantum processor. We also develop the first simulation of the energy calculation of the H<sub>2</sub> molecule using only a single qubit, and verify the results on an NMR quantum computer. Our experimental results demonstrate that only a single NMR qubit suffices to calculate the molecular energies of the H<sub>2</sub> molecule to the desired accuracy.

## I. INTRODUCTION

The current century is witnessing what is termed as the “second quantum revolution” and quantum computing is at its forefront [1]. In recent years, it has been shown that there are a number of problems that a quantum algorithm would solve much more efficiently as compared to its classical counterpart [2]. One such class of problems is ‘quantum simulation’, wherein the goal is to simulate a quantum system efficiently and gain the maximum amount of information about the system [3].

A major class of problems coming under the umbrella of quantum simulation[4] is the problem of finding the eigenstates of the Hamiltonian of a given system, which has been a prime focus in the field of quantum chemistry [5]. Finding the ground and excited state energies of a molecule gives enormous information about its properties, such as its stability, rate of reactions and the molecular orbitals involved [6]. The calculation of ground and excited state energies of molecules is of great importance in chemistry, but this becomes a challenging task for a classical computer as the complexity of the molecules grows. These problems are extremely difficult to solve analytically and hence the only way out is a numerical approach. However, even this becomes a daunting task for molecules with a large number of atoms and electrons, due to the large number of degrees of freedom involved. This is where quantum algorithms demonstrate their supremacy over their classical counterparts, and various quantum algorithms have been developed to efficiently calculate the energies of molecules on a quantum computer [7–9].

Quantum algorithms are prone to a lot of errors and require quantum error correction which limits their useful-

ness. Taking into consideration that we are in the NISQ era [10], a new class of algorithms has been developed, which are partly classical and partly quantum, which can reduce the required gate depth and mitigate errors to a certain extent. Variational Quantum Eigensolver (VQE) is one such algorithm that has been developed to calculate the ground state of Hamiltonians on a quantum computer [11–14]. The VQE algorithm may enable near-term quantum-enhanced computation [15] due to its low circuit depth.

In addition to ground state energy calculation of molecules, the excited state energies have several important applications. There have been a few proposals to develop an algorithm for the detection of excited states of a molecular Hamiltonian: a method that minimizes the von Neumann entropy [16] and the quantum subspace expansion method [17]. Recently, an algorithm which is an extension of the VQE algorithm was proposed, namely the Variational Quantum Deflation (VQD) algorithm, to calculate the excited state energies of molecules [18]. The VQD algorithm systematically finds excited states at almost no extra cost as compared to the other two methods. Using the VQD algorithm, the excited states are obtained by applying the VQE algorithm to a modified Hamiltonian which has the excited states as its ground state. Several experiments has been performed to demonstrate the energy spectra of molecules using VQE algorithms on different quantum platforms such as photonic quantum processors, trapped ions and using superconducting qubits [19–23].

In this paper, we have simulated the ground state energy and excited state energies of the H<sub>2</sub> molecule using the VQE and VQD algorithms, respectively. The simulated results are then verified on an NMR quantum processor. To use the variational principle, we varied the states in the qubit space so as to find the state which minimizes the energy expectation value. This is done by using the technique of Unitary Coupled Cluster Singles and Doubles (UCCSD) [24]. The experimental verification is done by calculating the expectation values terms

\* dsingh.iisermohali@gmail.com

† shashank.mehendale@mail.utoronto.ca

‡ arvind@iisermohali.ac.in

§ kavita@iisermohali.ac.in

involved in the  $H_2$  molecule Hamiltonian by using two NMR qubits. The experimental verification involves the calculation of expectation values of the state, and this is achieved by measuring the single-qubit Pauli  $Z$  operator of the experimentally prepared states. We also simulated the energies of the  $H_2$  molecule on a single qubit system and verified the results on an NMR quantum computer. This is the first experimental demonstration of energy calculations of the  $H_2$  molecule which requires only one qubit and uses fewer experimental resources as compared to similar work.

The material of the paper is arranged as follows: Section II describes the theoretical background of the variational quantum eigensolver algorithm, the variational quantum deflation algorithm, the electronic structure of  $H_2$  molecule and the solution of the  $H_2$  molecular Hamiltonian using one and two qubits. Section III describes the NMR implementation of the ground and excited state energies of the  $H_2$  molecule using a two-qubit and a single-qubit system, respectively. Section IV contains a few concluding remarks.

## II. THEORETICAL BACKGROUND

### A. Quantum variational methods for energy calculations

Given that quantum systems are described by Hamiltonians, finding their eigenvalues and eigenvectors is of paramount importance and becomes increasingly difficult with increase in system dimensionality. For a Hamiltonian  $H$ , an ansatz state  $|\psi(\theta)\rangle$  is chosen with at least one free parameter  $\theta$ . The expectation value of energy  $\epsilon_\theta = \langle \psi(\theta) | H | \psi(\theta) \rangle$  is minimized over the parameter  $\theta$  to obtain the minimum possible energy. The lowest expectation value that can be obtained in this way is the ground state energy of the Hamiltonian itself. In that case, the state  $|\psi(\theta)\rangle$  will be the ground state of the given Hamiltonian. However, this may not work as the family of states  $|\psi(\theta)\rangle$  may not contain the ground state! Therefore, a good choice of ansatz is important. On a quantum computer, there is an additional possibility of storing the quantum state in the quantum memory and carrying out the entire optimization process as a quantum computing process. The above variational VQE algorithm is a hybrid one, because a classical computer is used to update the value of the parameter  $\theta$  [11].

A variation of the above method can be used to calculate the excited states of the Hamiltonian and the procedure is called the VQD method [18]. If  $|\phi_0\rangle$  is the ground state of the original Hamiltonian  $H$ , the VQD Hamiltonian for the first excited state is given by:

$$H_1 = H + \beta_0 |\phi_0\rangle \langle \phi_0| \quad (1)$$

where  $\beta_0$  is a parameter and is chosen such that the variational calculation applied on  $H_1$  gives its minimum energy (such that it is equal to the first excited state of of

the original Hamiltonian  $H$ ). The VQD method can be easily extended to find the other excited states of  $H$  by appropriately constructing the new Hamiltonian for the variational purpose.

### B. Solving for energies of the $H_2$ molecule

The Hamiltonian of the  $H_2$  molecule in atomic units is given by [17, 19]:

$$H = - \sum_i \frac{\nabla_{R_i}}{2M_i} - \sum_i \frac{\nabla_{r_i}}{2} + \sum_{i,j>i} \frac{Z_i Z_j}{|R_i - R_j|} - \sum_{i,j>i} \frac{Z_i}{|R_i - r_j|} + \sum_{i,j>i} \frac{1}{|r_i - r_j|} \quad (2)$$

where  $R_i, M_i, Z_i$  denote the position, mass and charge of the  $i^{\text{th}}$  nuclei respectively, and  $r_i$  denotes the position of the  $i^{\text{th}}$  electron.

The above Hamiltonian is first solved in the Born-Oppenheimer approximation and then cast into the second quantized form using a specific choice of  $N$ -particle basis functions [19]. Since quantum many-body problems are described in the language of second quantization, one needs a formalism to translate the language of second quantization to a language that a quantum computer can read. This can be achieved in various ways, including the Jordan-Wigner transformation, the Bravyi-Kitaev transformation, and the Parity transformation [19]. In this work, we use the Parity transformation. The quantum many-body Hamiltonian can be written in second quantization as [19]:

$$H = \sum_{\mu,\nu} t_{\mu,\nu} c_\mu^\dagger c_\nu + \sum_{\mu,\nu,\mu',\nu'} V_{\mu,\nu,\mu',\nu'} c_\mu^\dagger c_\nu^\dagger c_{\nu'} c_{\mu'}$$

where,

$$t_{\mu,\nu} = \int d\sigma \phi_\mu^*(\sigma) \left( -\frac{\nabla_r}{2} - \sum_i \frac{Z_i}{|R_i - r|} \right) \phi_\nu(\sigma)$$

$$V_{\mu,\nu,\mu',\nu'} = \int d\sigma_1 d\sigma_2 \frac{\phi_\mu^*(\sigma_1) \phi_\nu^*(\sigma_2) \phi_{\mu'}(\sigma_1) \phi_{\nu'}(\sigma_2)}{|r_1 - r_2|}$$

where  $\sigma_i = (r_i, s_i)$  with  $r_i, s_i$  are the position and spin indices, respectively. The operators  $c_\mu, c_\mu^\dagger$  are the lowering and raising operators for electron occupation in orbitals.

To solve the above Hamiltonian on a quantum computer using the VQD algorithm, all the second quantized operators have to be mapped to the Pauli operators, and the orbitals have to be mapped to qubits. Using the Parity transformation, the many-body  $H_2$  Hamiltonian is mapped to the qubit Hamiltonian acting in a two-qubit state space [25, 26]:

$$H = a_0 II + a_1 ZI + a_2 IZ + a_3 ZZ + a_4 XX \quad (3)$$

The coefficients  $a_i$  encode the information of molecular integrals pertaining to a specific basis set. We have chosen the STO-3G basis in our calculations. The Qiskit.Chemistry module [27] was used to generate the Hamiltonian in the STO-3G basis, which was then converted to a qubit Hamiltonian using the Parity map. The values of the  $a_i$  coefficients corresponding to each Pauli operator were extracted as a function of different inter-nuclear distances.

In order to use the variational principle for the minimum energy calculation, we use the Unitary Coupled Cluster Singles and Doubles (UCCSD) ansatz:

$$|\psi(\theta)\rangle = U(\theta)|\psi_0\rangle \quad (4)$$

where  $|\psi_0\rangle$  is an initial reference state and  $U(\theta)$  is the UCCSD evolution operator. The choice of the reference state is the Hartree-Fock (HF) state, which definitely has a support on the ground state of the Hamiltonian. After writing the HF state in the Parity basis, the symmetry in the action of UCCSD operator and the HF state can be exploited to give a two-qubit UCCSD operator:

$$U(\theta) = \exp(i\theta XY) \quad (5)$$

with the HF state given by  $|01\rangle$  [19]. The action of  $U(\theta)$  on  $|01\rangle$  can be computed from:

$$U(\theta)|01\rangle = \exp(i\theta XY)|01\rangle = \cos\theta|01\rangle + \sin\theta|10\rangle \quad (6)$$

The action of  $U(\theta)$  on  $|01\rangle$ , and then minimization of the energy expectation leads to the ground state of the Hamiltonian. The classical minimization process is done using the Nelder-Mead method given by the minimize function of the *scipy.optimize* module [28, 29]. The VQD modified Hamiltonian and the same ansatz leads to an excited state of the  $H_2$  molecule.

Given that we obtained two energy eigenstates of the Hamiltonian in the space spanned by the vectors  $|01\rangle, |10\rangle$ , the other two eigenstates belong to the space spanned by the other two computational basis vectors, namely  $|00\rangle$  and  $|11\rangle$ . In order to find the other two eigenstates, we take the initial state to be  $|00\rangle$ , and apply the ansatz circuit which performs the evolution  $U(\theta)$  (as in the previous case) given by:

$$U(\theta) = \exp(i\theta XY)U(\theta)|00\rangle = \cos\theta|00\rangle - \sin\theta|11\rangle \quad (7)$$

Since the  $H_2$  Hamiltonian of Eqn. (3) is real in the computational basis, there has to exist a real eigenbasis for the Hamiltonian with real coefficients of expansion in the computational basis. Thus, we do not have to explore the space where the relative phase between the two computational basis vectors is complex. Hence the problem essentially gets divided into two problems, each of two dimensions.

### C. Solving for the energies of the $H_2$ molecule using a single qubit

As is clear from Equation 6 in the previous section, the UCCSD ansatz only explores a two-dimensional sub-

TABLE I. The action of the individual terms of the Hamiltonian on the states  $|01\rangle$  and  $|10\rangle$ .

$II 01\rangle$	$=$	$ 01\rangle$	$II 10\rangle$	$=$	$ 10\rangle$
$ZI 01\rangle$	$=$	$ 01\rangle$	$ZI 10\rangle$	$=$	$- 10\rangle$
$IZ 01\rangle$	$=$	$- 01\rangle$	$IZ 10\rangle$	$=$	$ 10\rangle$
$ZZ 01\rangle$	$=$	$- 01\rangle$	$ZZ 10\rangle$	$=$	$- 10\rangle$
$XX 01\rangle$	$=$	$ 10\rangle$	$XX 10\rangle$	$=$	$ 01\rangle$

space of the entire four-dimensional space. This creates a possibility of mapping the two-dimensional subspace to a single-qubit space. If we map the state to involved to a single-qubit state as:

$$|01\rangle \rightarrow |0\rangle, \text{ and } |10\rangle \rightarrow |1\rangle \quad (8)$$

the UCCSD operator gets mapped to  $\exp(-i\theta Y)$ , where  $Y$  acts on the single-qubit space.

In order to map the Hamiltonian, we first evaluate how different terms of the Hamiltonian act on the basis vectors spanning the subspace (Table I).

It is evidence from Table I, that:

$$\begin{aligned} II &\longrightarrow I & ZZ &\longrightarrow -I \\ ZI &\longrightarrow Z & IZ &\longrightarrow -Z \\ XX &\longrightarrow X \end{aligned} \quad (9)$$

Thus, the diagonalization of the Hamiltonian in the two-dimensional subspace of the two-qubit space reduces to the diagonalization of a single-qubit Hamiltonian given by:

$$H = (a_0 - a_3)I + (a_1 - a_2)Z + a_4X \quad (10)$$

with the UCCSD ansatz  $\exp(-i\theta Y)$  and the initial state  $|0\rangle$ .

For the remaining two eigenstates, we follow an analogous procedure to obtain:

$$H = (a_0 + a_3)I + (a_1 + a_2)Z + a_4X \quad (11)$$

with the UCCSD ansatz  $\exp(i\theta Y)$  and the initial state  $|0\rangle$ .

Diagonalizing these two Hamiltonians will give all the four excited states of the original two-qubit  $H_2$  Hamiltonian. The reduction of the problem to a single qubit is resource efficient from the point of view of its experimental implementation. Further, since there are only three terms in the Hamiltonian, the calculation of energy expectation values becomes simpler. Additionally, the UCCSD ansatz, unlike in the two-qubit qubit case, is now a simple rotation about the  $Y$ -axis, which is easier to implement experimentally on any quantum platform. Last but not the least, the initial state can be directly taken to be the pseudopure state on an NMR quantum computer, without any additional requirement to prepare

a reference state. With all these advantages, we have shown that the entire problem of diagonalization of the two-qubit  $H_2$  molecule can be easily recast as a problem of diagonalization in a single-qubit space.

### III. EXPERIMENTAL IMPLEMENTATION

#### A. Calculating energies of the $H_2$ molecule using two NMR qubits

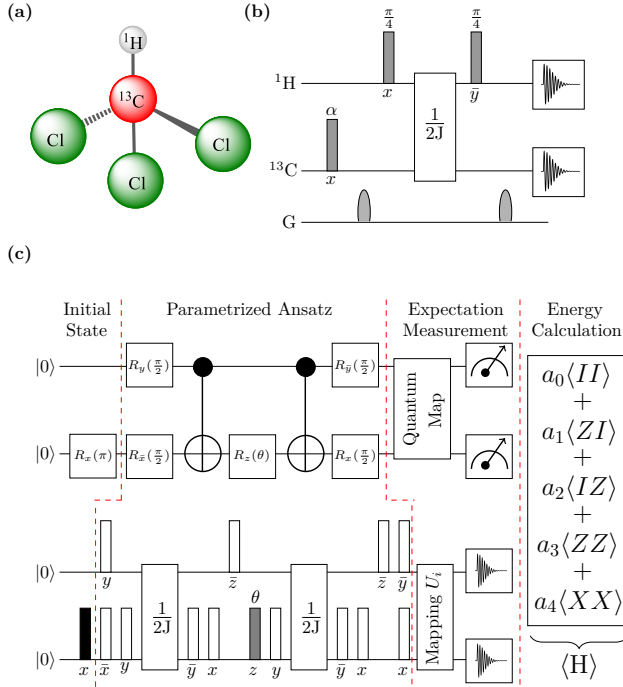


FIG. 1. (a) Molecular structure of  $^{13}\text{C}$ -labeled chloroform used as a two-qubit quantum system. (b) NMR pulse sequence for the PPS  $|00\rangle$  state where the value of the flip angle  $\alpha$  is kept fixed at  $59.69^\circ$ , while  $J$  represents the coupling between the  $^1\text{H}$  and  $^{13}\text{C}$ ; the total time evolution is given by  $\frac{1}{2J}$ . (c) Quantum circuit for the required state, generated with an optimized value of  $\theta$  for different intermolecular distances. The unfilled rectangles denote  $\pi$  pulses, while the filled rectangle represents a  $\frac{\pi}{2}$  pulse. The flip angles and phases of the other pulses are written below each pulse, and a bar over the phase denotes negative phase.

To experimentally calculate the energies simulated by VQE algorithms of the  $H_2$  molecule on a four-dimensional quantum system, the molecule of  $^{13}\text{C}$  enriched chloroform dissolved in acetone- $D_6$  was used, with the  $^{13}\text{C}$  and  $^1\text{H}$  spins being labeled as qubit 1 and qubit 2, respectively (Fig. 1(a)). NMR experiments are sensitive only to the deviation density matrix and the initial state is typically prepared from thermal equilibrium as a pseudo-pure state (PPS), which mimics the evolution of true

pure states [30]:

$$\rho_{00} = \frac{1-\epsilon}{2^3} I_4 + \epsilon |00\rangle\langle 00| \quad (12)$$

where spin polarization  $\epsilon \approx 10^{-6}$  and  $I_4$  is the  $4 \times 4$  identity operator. We initialized the system in the PPS  $|00\rangle$  using the spatial averaging technique [30], via a combination of RF pulses and pulsed magnetic gradients. The NMR pulse sequence for the PPS is given in Fig. 1(b).

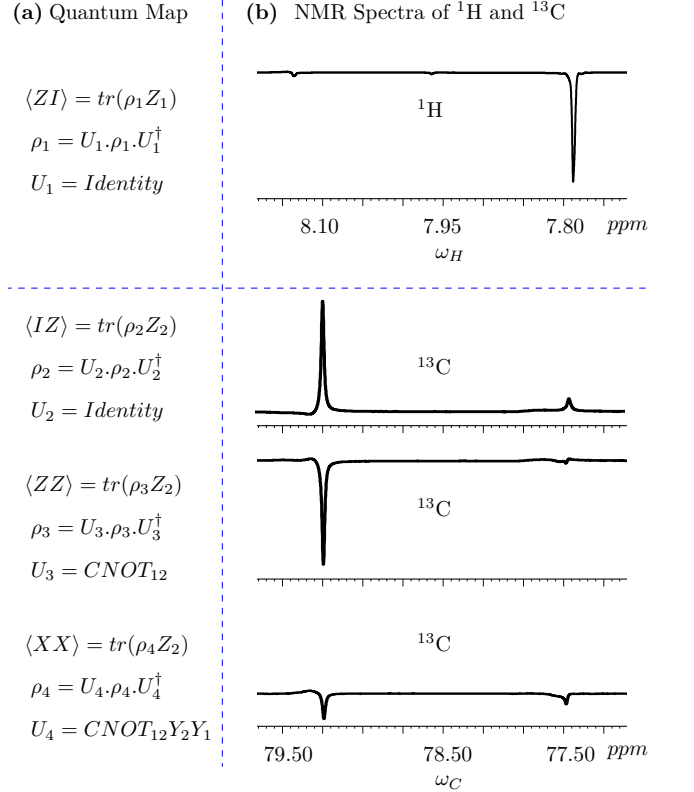


FIG. 2. (a) Details of the mapping performed for the measurement of the expectation values  $\langle ZI \rangle$ ,  $\langle IZ \rangle$ ,  $\langle ZZ \rangle$ ,  $\langle XX \rangle$ . The Identity operator  $I$  denotes 'no operation'. (b) NMR spectra of  $^1\text{H}$  and  $^{13}\text{C}$ , displaying the experimentally measured expectation values of  $\langle ZI \rangle$  and  $\langle IZ \rangle$ ,  $\langle ZZ \rangle$ ,  $\langle XX \rangle$ , respectively, for the ground state energy calculation, at an intermolecular distance  $R = 0.70 \text{ \AA}$ .

Experiments were performed on a Bruker Avance III 600-MHz FT-NMR spectrometer equipped with a TXI probe. Quantum gates, required for the NMR implementation, were achieved by using specially crafted RF pulses of suitable amplitude, phase, and duration and nonlocal unitary operations were achieved by free evolution under the system Hamiltonian. The  $T_1$  and  $T_2$  relaxation times of the  $^1\text{H}$  spin-1/2 nuclei were  $\approx 8 \text{ sec}$  and  $\approx 3 \text{ sec}$ , respectively. The  $T_1$  and  $T_2$  relaxation times of the  $^{13}\text{C}$  spin-1/2 nuclei were  $\approx 17 \text{ sec}$  and  $\approx 0.5 \text{ sec}$ , respectively. The duration of the  $\frac{\pi}{2}$  pulses for  $^1\text{H}$  and  $^{13}\text{C}$  nuclei were  $7.14 \mu\text{s}$  at a power level of  $19.9 \text{ W}$ , and  $12.4 \mu\text{s}$  at a power level of  $237.3 \text{ W}$ , respectively.

TABLE II. Hamiltonian coefficients  $a_i, i = 0, 1, 2, 3, 4$  for different internuclear separations (R).

R (Å)	$a_0$	$a_1$	$a_2$	$a_3$	$a_4$
0.30	-0.75374	0.80864	-0.80864	-0.01328	0.16081
0.40	-0.86257	0.68881	-0.68881	-0.01291	0.16451
0.50	-0.94770	0.58307	-0.58307	-0.01251	0.16887
0.60	-1.00712	0.49401	-0.49401	-0.01206	0.17373
0.70	-1.04391	0.42045	-0.42045	-0.01150	0.179005
0.80	-1.06321	0.35995	-0.35995	-0.01080	0.18462
0.90	-1.07028	0.30978	-0.30978	-0.00996	0.19057
1.00	-1.06924	0.26752	-0.26752	-0.00901	0.19679
1.10	-1.06281	0.23139	-0.23139	-0.00799	0.20322
1.20	-1.05267	0.20018	-0.20018	-0.00696	0.20979
1.30	-1.03991	0.17310	-0.17310	-0.00596	0.21641
1.40	-1.02535	0.14956	-0.14956	-0.00503	0.22302
1.50	-1.00964	0.12910	-0.12910	-0.00418	0.22953
1.60	-0.99329	0.11130	-0.11130	-0.00344	0.23590
1.70	-0.97673	0.09584	-0.09584	-0.00280	0.24207
1.80	-0.96028	0.08240	-0.08240	-0.00226	0.24801

In order to experimentally calculate the energies of the  $H_2$  molecule, we need to calculate the expectation values of  $\langle ZI \rangle$ ,  $\langle IZ \rangle$ ,  $\langle ZZ \rangle$ ,  $\langle XX \rangle$ . In an NMR experiment these expectation values can be calculated by mapping them onto the single-qubit Pauli  $Z$  operator. This mapping is easily performed in the context of an NMR experimental measurement as the observed  $z$  magnetization of a nuclear spin in a particular quantum state is proportional to the expectation value of the Pauli  $Z$  operator of the spin in that state [31, 32]. For instance, in order to determine the expectation value  $\langle ZZ \rangle$  for the state  $\rho = |\psi\rangle\langle\psi|$ , we map the state  $\rho$  to  $\rho_1 = U_1\rho U_1^\dagger$ , where  $U_1 = \text{CNOT}_{12}$  followed by observing  $\langle Z_2 \rangle$  for the state  $\rho_1$ . The expectation value of  $\langle Z_2 \rangle$  for the state  $\rho_1$  is equivalent to observing the expectation value of  $\langle ZZ \rangle$  for the state  $\rho$ .

The quantum circuit and corresponding NMR pulse sequence for the experimental calculation of required expectation values is given in Fig. 1(c). The circuit comprises three parts (delineated by dashed red lines in Fig. 1(c)): the first part corresponds to initializing the state to the HF state  $|01\rangle$ , which is achieved by applying a single-qubit rotation on the  $|00\rangle$  state. The second part of the circuit applies the parameterized ansatz  $U(\theta)$  on the initial state, which is achieved by optimizing the value of  $\theta$  (using the Nelder-Mead method and

the *scipy.optimize* module). The third part of the circuit calculates the expectation values  $\langle ZI \rangle$ ,  $\langle IZ \rangle$ ,  $\langle ZZ \rangle$ ,  $\langle XX \rangle$  for the parameterized ansatz, which is achieved by mapping these expectation values onto the single-qubit Pauli  $Z$  operator. The experimentally calculated energies are obtained by adding these expectation values to their respective electronic constants ( $a_i, i = 0, 1, 2, 3, 4$ ). The numerical values of the electronic constants are tabulated in Table II, for different values of the internuclear separation (R) of the  $H_2$  molecule.

The ground state and the excited state energies of the  $H_2$  molecule were experimentally calculated using VQE and VQD algorithms, respectively, for sixteen different internuclear distances in the range 0.30–1.80 Å. For each of these internuclear separations, there are five associated electronic constants  $a_0, a_1, a_2, a_3, a_4$  (as given in the  $H_2$  molecular Hamiltonian in Eqn. (3)). Fig. 2(a) contains the details of mapping that we have used in the NMR experiment to calculate the expectation values required for the experimentally prepared states. Fig. 2(b) depicts the NMR spectra of the expectation values  $\langle ZI \rangle$ ,  $\langle IZ \rangle$ ,  $\langle ZZ \rangle$ ,  $\langle XX \rangle$  for the ground state energy at an internuclear separation of  $R = 0.70$  Å. The ground and excited state energies of the  $H_2$  molecule have been experimentally calculated using a similar method, for the thirteen other internuclear separations. The ground and excited

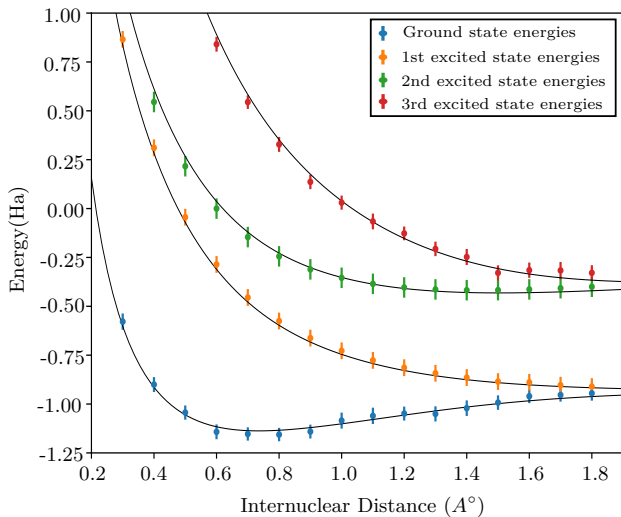


FIG. 3. Ground and excited state energies of the  $H_2$  molecule calculated using the VQE and VQD algorithms, respectively, over a range of internuclear separations. The simulated results are represented by joined lines, while the experimentally calculated values (obtained using two NMR qubits) are represented by distinct points with accompanying error bars.

state energies have been plotted as a function of the internuclear distances in Fig. 3. As evident from the plot in Fig. 3, the simulated and experimentally measured values agree well, to within experimental errors.

### B. Calculating energies of the $H_2$ molecule using one NMR qubit

To experimentally calculate the energies of the  $H_2$  molecule via variational quantum algorithms implemented on a two-dimensional quantum system, the molecule of chloroform dissolved in acetone- $D_6$  was used, with the  $^1H$  spin realizing a single qubit (Fig. 4(a)). In order to perform the energy calculation, we need to calculate only two expectation values, namely  $\langle Z \rangle$  and  $\langle X \rangle$ . The details of the mapping used for the experimental calculation are given in Fig. 4(b). Fig. 4(c), depicts the NMR spectra of the expectation values of  $\langle Z \rangle$ ,  $\langle X \rangle$  for the ground state energy of the  $H_2$  molecule at the internuclear separation  $R = 0.70 \text{ \AA}$ .

The ground and excited state energies for the  $H_2$  molecule have been calculated experimentally for sixteen different internuclear separations. The ground and excited state energies have been plotted as a function of the internuclear separation in Fig. 5. The red dashed curve represents the energy calculation corresponding to the reduced single-qubit Hamiltonian given in Eqn. (10). The green curve represents the energy calculation corresponding to the reduced single-qubit Hamiltonian given in Eqn. (11). As is evident from the plot in Fig. 5, the simulated and experimentally measured values agree well to within experimental errors. Furthermore, it is remark-

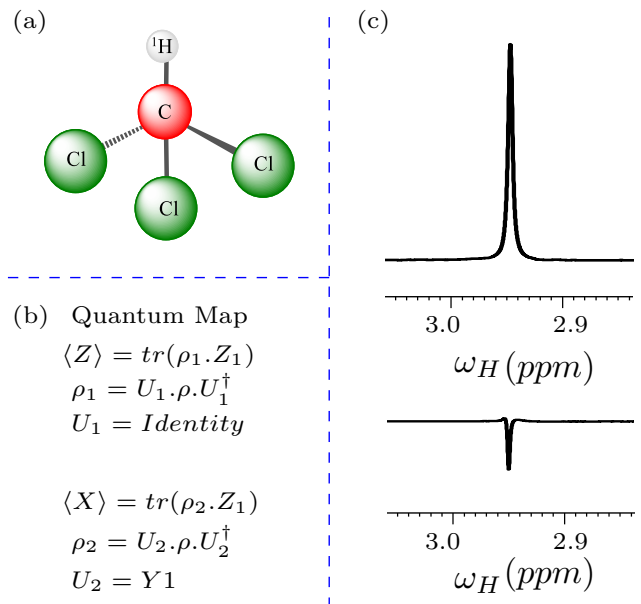


FIG. 4. (a) Molecular structure of chloroform, used as a one-qubit quantum system. (b) Mapping details for the measurement of the expectation values  $\langle Z \rangle$  and  $\langle X \rangle$ . The identity operator  $I$  denotes ‘no operation’. (c) NMR spectra of  $^1H$ , depicting the experimentally measured expectation values of  $\langle Z \rangle$  and  $\langle X \rangle$ .

able that the simulated and experimentally measured values of the molecular energies in Fig. 5, are very close to the values obtained in Fig. 3, validating the efficiency of the VQD algorithm using only a single qubit.

The experimental complexity is reduced due to the reduction of two-qubit system to a one-qubit system. We were hence able to calculate the energy spectra of the  $H_2$  molecule by measuring only two expectation values, namely,  $\langle Z \rangle$  and  $\langle X \rangle$ . In the corresponding NMR experiments, these expectation values can be obtained by applying a single RF pulse on the experimentally prepared state. This is the first experimental demonstration on an NMR quantum simulator of the calculation of energies of the  $H_2$  molecule which requires only a single qubit for its implementation.

## IV. CONCLUSIONS

The ground and excited states of the  $H_2$  Hamiltonian were obtained in the Parity basis using VQE and VQD algorithms, and the results of the calculations were verified on an NMR quantum simulator. Further, the problem of calculation of the  $H_2$  ground state energy was reduced to a single-qubit problem which was also verified on the NMR quantum simulator. Two NMR qubits were used for the simulation of the single-qubit problem and the expectation values involved in the Hamiltonian were obtained by measuring the single-qubit Pauli  $Z$  operator of the experimentally prepared state. The experimental

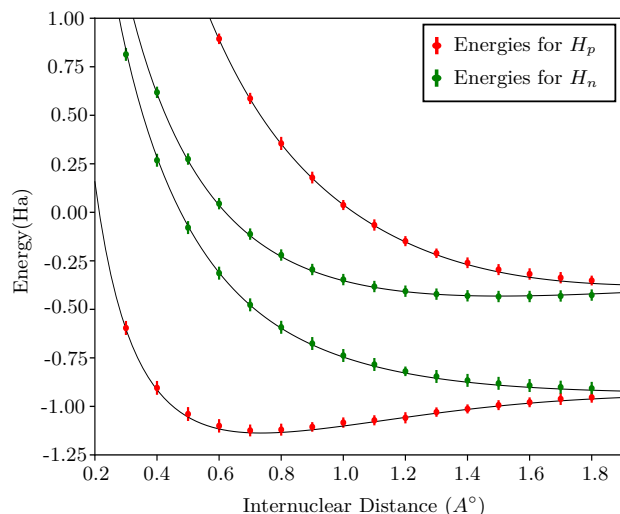


FIG. 5. Simulations and experimental calculations of the ground and excited state energies of the  $H_2$  molecule, for a range of internuclear separations. The simulated results are represented by joined lines, while the experimentally calculated values (obtained using a single NMR qubit) are represented by distinct points with accompanying error bars.

implementation of variational quantum algorithms to calculate the ground and excited state energies of molecules is important for the field of quantum chemistry, and our results are a step forward in this direction.

## ACKNOWLEDGMENTS

All the experiments were performed on a Bruker Avance-III 600 MHz FT-NMR spectrometer at the NMR Research Facility of IISER Mohali. A. acknowledges financial support from DST/ICPS/QuST/Theme-1/2019/Q-68. K.D. acknowledges financial support from DST/ICPS/QuST/Theme-2/2019/Q-74.

- 
- [1] A. G. J. MacFarlane, J. P. Dowling, and G. J. Milburn, *Philos. Trans. R. Soc. London. Ser. A* **361**, 1655 (2003).
- [2] M. A. Nielsen and I. L. Chuang, *Quantum Computation and Quantum Information* (Cambridge University Press, Cambridge UK, 2010).
- [3] R. P. Feynman, *Int. J. Theor. Phys.* **21**, 467 (1982).
- [4] S. Lloyd, *Science* **273**, 1073 (1996).
- [5] Y. Cao, J. Romero, J. P. Olson, M. Degroote, P. D. Johnson, M. Kieferová, I. D. Kivlichan, T. Menke, B. Peropadre, N. P. D. Sawaya, S. Sim, L. Veis, and A. Aspuru-Guzik, *Chem. Rev.* **119**, 10856 (2019), pMID: 31469277, <https://doi.org/10.1021/acs.chemrev.8b00803>.
- [6] A. Aspuru-Guzik, A. D. Dutoi, P. J. Love, and M. Head-Gordon, *Science* **309**, 1704 (2005).
- [7] J. D. Whitfield, J. Biamonte, and A. Aspuru-Guzik, *Mol. Phys.* **109**, 735 (2011), <https://doi.org/10.1080/00268976.2011.552441>.
- [8] I. Kassal, J. D. Whitfield, A. Perdomo-Ortiz, M.-H. Yung, and A. Aspuru-Guzik, *Annu. Rev. Phys. Chem.* **62**, 185 (2011), pMID: 21166541, <https://doi.org/10.1146/annurev-physchem-032210-103512>.
- [9] N. C. Jones, J. D. Whitfield, P. L. McMahon, M.-H. Yung, R. V. Meter, A. Aspuru-Guzik, and Y. Yamamoto, *New J. Phys.* **14**, 115023 (2012).
- [10] J. Preskill, *Quantum* **2**, 79 (2018).
- [11] J. R. McClean, J. Romero, R. Babbush, and A. Aspuru-Guzik, *New J. Phys.* **18**, 023023 (2016).
- [12] N. Moll, P. Barkoutsos, L. S. Bishop, J. M. Chow, A. Cross, D. J. Egger, S. Filipp, A. Fuhrer, J. M. Gambetta, M. Ganzhorn, A. Kandala, A. Mezzacapo, P. Müller, W. Riess, G. Salis, J. Smolin, I. Tavernelli, and K. Temme, *Quantum Sci. Technol.* **3**, 030503 (2018).
- [13] T. Jones, S. Endo, S. McArdle, X. Yuan, and S. C. Benjamin, *Phys. Rev. A* **99**, 062304 (2019).
- [14] D. Wang, O. Higgott, and S. Brierley, *Phys. Rev. Lett.* **122**, 140504 (2019).
- [15] A. Peruzzo, J. McClean, P. Shadbolt, M.-H. Yung, X.-Q. Zhou, P. J. Love, A. Aspuru-Guzik, and J. L. O'Brien, *Nat. Commun.* **5**, 4213 (2014).
- [16] R. Santagati, J. Wang, A. A. Gentile, S. Paesani, N. Wiebe, J. R. McClean, S. Morley-Short, P. J. Shadbolt, D. Bonneau, J. W. Silverstone, D. P. Tew, X. Zhou, J. L. O'Brien, and M. G. Thompson, *Sci. Adv.* **4**, eaap9646 (2018).
- [17] J. I. Colless, V. V. Ramasesh, D. Dahlen, M. S. Blok, M. E. Kimchi-Schwartz, J. R. McClean, J. Carter, W. A. de Jong, and I. Siddiqi, *Phys. Rev. X* **8**, 011021 (2018).
- [18] O. Higgott, D. Wang, and S. Brierley, *Quantum* **3**, 156 (2019).
- [19] P. J. J. O'Malley, R. Babbush, I. D. Kivlichan, J. Romero, J. R. McClean, R. Barends, J. Kelly, P. Roushan, A. Tranter, N. Ding, B. Campbell, Y. Chen, Z. Chen, B. Chiaro, A. Dunsworth, A. G. Fowler, E. Jeffrey, E. Lucero, A. Megrant, J. Y. Mutus, M. Neeley, C. Neill, C. Quintana, D. Sank, A. Vainsencher, J. Wenner, T. C. White, P. V. Coveney, P. J. Love, H. Neven, A. Aspuru-Guzik, and J. M. Martinis, *Phys. Rev. X* **6**, 031007 (2016).
- [20] C. Hempel, C. Maier, J. Romero, J. McClean, T. Monz, H. Shen, P. Jurcevic, B. P. Lanyon, P. Love, R. Babbush, A. Aspuru-Guzik, R. Blatt, and C. F. Roos, *Phys. Rev. X* **8**, 031022 (2018).
- [21] M. Motta, G. O. Jones, J. E. Rice, T. P. Gujarati, R. Sakuma, I. Liepuoniute, J. M. Garcia, and Y.-y. Ohnishi, *Chem. Sci.* **14**, 2915 (2023).

- [22] M. A. Jones, H. J. Vallury, and L. C. Hollenberg, *Phys. Rev. Appl.* **21**, 064017 (2024).
- [23] J. P. Misiewicz and F. A. Evangelista, *J. Phys. Chem. A* **128**, 2220 (2024).
- [24] R. Xia and S. Kais, *Quantum Sci. Technol.* **6**, 015001 (2020).
- [25] J. T. Seeley, M. J. Richard, and P. J. Love, *J. Chem. Phys.* **137**, 224109 (2012), <https://doi.org/10.1063/1.4768229>.
- [26] M. Ganzhorn, D. Egger, P. Barkoutsos, P. Ollitrault, G. Salis, N. Moll, M. Roth, A. Fuhrer, P. Mueller, S. Woerner, I. Tavernelli, and S. Filipp, *Phys. Rev. Applied* **11**, 044092 (2019).
- [27] A. Javadi-Abhari, M. Treinish, K. Krsulich, C. J. Wood, J. Lishman, J. Gacon, S. Martiel, P. D. Nation, L. S. Bishop, A. W. Cross, B. R. Johnson, and J. M. Gambetta, “Quantum computing with Qiskit,” (2024), arXiv:2405.08810 [quant-ph].
- [28] D. M. Olsson and L. S. Nelson, *Technometrics* **17**, 45 (1975).
- [29] T. S. community, “scipy.optimize,” (2008-2024).
- [30] I. S. Oliveira, T. J. Bonagamba, R. S. Sarthour, J. C. C. Freitas, and E. R. deAzevedo, *NMR Quantum Information Processing* (Elsevier, Linacre House, Jordan Hill, Oxford OX2 8DP, UK, 2007).
- [31] A. Gaikwad, D. Rehal, A. Singh, Arvind, and K. Dorai, *Phys. Rev. A* **97**, 022311 (2018).
- [32] D. Singh, J. Singh, K. Dorai, and Arvind, *Phys. Rev. A* **100**, 022109 (2019).